BIFURCATION ANALYSIS OF A TWO-DIMENSIONAL BINARY MIXTURE OF HARD NEEDLES

Agnieszka Chrzanowska

Institute of Physics, Kraków University of Technology
Podchorążych 1, 30-084 Kraków, Poland
achrzano@usk.pk.edu.pl

(Received November 19, 2012)

Bifurcation analysis of a two-dimensional binary mixture of hard needles, which due to the second order of the transition character gives directly the density of the transitions, thus the phase diagram, has been performed for a complete set of the compositions and the needles lengths ratios within the framework of the Onsager approach. A limit of a mixture of needles and dot-like particles has been given. The possible changes in the phase diagrams caused by modification of the interaction strength of the different type particles are discussed. Prognosis of applications for the surfacial adsorption of the rod-type molecules like fibrinogen has been suggested.

DOI:10.5506/APhysPolB.44.91
PACS numbers: 71.15.Mb, 64.70.Md, 61.30.–v

1. Introduction

Two-dimensional systems are peculiar for many reasons. They are less popular than three-dimensional systems, nevertheless new technical applications of adsorption at solid surfaces cause that interest in such systems is on the increase.

One of the peculiarities is the existence of the so-called topological long range order. Most 2D systems that exhibit continuous degrees of freedom lack true long-range order (LRO), *i.e.* the order that pertains throughout the whole system. Topological order, which name has been used for the first time by Kosterlitz and Thouless in [1], describes the case when a well defined order pertains, more or less constantly, over several particles' dimensions, but as the system size is increased, it diminishes and reaches zero value for infinitely large systems. Thus, on the one side, on the short distance scale there is an ordered system, on the other side, for infinitely large systems — there is no long range order. Such type of ordering follows from harmonic or continuous

theories [1–4] and has been also demonstrated on the basis of the Bogoliubov inequality for superconductors, superfluids, magnets, translational order in crystals [5] and certain classes of liquid crystals [6].

Despite the lack of long range order, mechanical or physical properties of thin films or two-dimensional adsorbed layers may strongly depend on the short range ordering properties. The fact that ordering can have considerable impact on covering layers is already widely known [7, 8]. More complex structures with hard needles like nets can serve as a model for liquid-crystal polymer mixtures [9]. Additional effects occur when the adsorbed particles are not spherical. Hence, it rises strong motivation for exploration of such materials.

In the case of anisotropic particles, there exist a number of theoretical tools, emerging mainly from the liquid crystals field, that allow to predict and describe the physical states of the systems. The most powerful approach are different types of the density functional theories (DFT). For hard bodies it takes the form of the Onsager theory, which in the case of thick particles requires amendments like the Parsons Lee re-scaling [10, 11] or y-expansion of Barboy and Gelbart [12].

In the case of hard needles, which are the subject of the present paper study, the situation is different. While studying the monodispersed system of hard needles it has turned out, surprisingly, that the transition point of the isotropic–nematic transition and the obtained state equation from the Onsager approach are almost the same as those predicted from the computer simulations [13–16] for a small and undistorted system. Such a result is attributed to the presence of negative values of the higher virial coefficients, which may cancel the influence of the other positive coefficients in such a way that the second order virial approximation gives accurate predictions. There is then a real chance that the results of the other DFT models with hard needles can be directly used to judge about the physical properties.

Hard needles is the system which has been widely studied so far, both by the DFT approaches [16–21] and the computer simulations [13, 15, 22–27]. The main benefit of studying this model is the easiness to understand the mechanisms that lead to different properties, especially useful since the needles form a natural limit for all anisotropic bodies — they can be obtained by diminishing the width of spherocylinders, ellipsoids or other shapes. In view of this, the hard needles properties can be used for comparison with the properties of the systems where particles exhibit large values of the length to breadth ratio. This conclusion does not hold as a whole for 3D case where the hard needles do no form orientationally ordered phases, but can work very well within the 2D assumption [28].

The present paper provides the Onsager formalism for a binary mixture of 2D hard needles, the possible phase diagrams from the bifurcation analysis and emerging from it conclusions. The paper is organized as follows. The next section presents the elements of the density functional theory within the Onsager approach for a two-dimensional mixture: the excluded volume of 2D needles, the free energy of a 2D mesogenic mixture and the formulas for the self-consistency equations and pressure. Section 3 presents bifurcation analysis and in Sec. 4 the results, applications and perspectives are discussed.

2. Density functional theory

The DFT approach is a common and a relatively simple theoretical tool which allows to calculate the equilibrium states of the system particles. Its main element is the Helmholtz free energy functional which is expected to attain minimum for the equilibrium distribution function. In the case of hard particles, the interaction terms in the energy are governed by the excluded volume. The minimization procedure gives self-consistent equations for the density distribution which must be numerically solved. Knowing these solutions all thermodynamic properties like pressure, energy or chemical potential can be obtained. For hard bodies it takes the form of the Onsager theory [29].

2.1. Excluded volume of 2D needles

In the case of hard bodies, the excluded volume plays the role of interactions. In general, it is defined as a set of points in space, which are not accessible to the center of the other body. It is obtained while the other body with fixed orientation is being moved around the central particle. For the two-dimensional case of hard needles, it corresponds to the parallelogram area with the sides equal to the lengths of the needles and tilted at the angle ϕ. In Fig. 1, it is given by the shadowed area. Here, the central

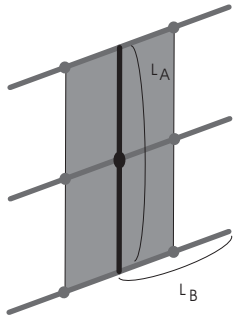

Fig. 1. The 2D excluded volume of two different hard needles.

needle is painted as black and the needle moving around is gray. This area is given by the formula

$$V_{\text{excl}} = L_A L_B |\sin(\phi)|\,, \tag{1}$$

where L_A and L_B are the lengths of the molecules A and B.

2.2. The free energy of a 2D mesogenic mixture

The total energy of the nematic system F_{tot} can be given, in general, as a sum of the following terms

$$F_{\text{tot}} = F_{\text{uni}} + F_{\text{elastic}} + F_{\text{exter}} + F_{\text{defects}}\,, \tag{2}$$

where F_{uni} describes the energy of the uniform system, F_{elastic} is the elastic energy due to the director deformations, F_{exter} is the energy of the system interactions with external fields and F_{defects} corresponds to the energy of the possible defects. The first term is the most fundamental for liquid crystals. It can be directly compared to the simulation data if the simulated system is small enough to ensure that the director is undeformed and there are no disclinations.

The Helmholtz free energy functional [30] that describes a binary mixture in the second order virial approximation takes the form

$$\begin{aligned}\beta F = \beta F_0 &+ \int \rho_A(1)\,(log\rho_A(1) - 1)\;\, d(1) + \int \rho_B(1)\,(log\rho_B(1) - 1)\;\, d(1) \\ &- \sum_{i,j=A,B} \tfrac{1}{2} \int \left[e^{-\beta U_{ij}} - 1\right] \rho_i(1)\rho_j(2) d(1) d(2)\,,\end{aligned} \tag{3}$$

where $(1) \equiv d\boldsymbol{r}_1 d\phi_1$. F_0 can comprise as well the de Broglie wavelength term as any shift determined by the choice of the zero level of energy. The distribution ρ_i is normalized to the total number of particles N_i of a given type i as follows

$$\int \rho_i(\boldsymbol{r}_1, \phi_1) d\boldsymbol{r}_1 d\phi_1 = N_i\,. \tag{4}$$

For the system homogeneous in space, we can introduce a proper probabilistic function $f_i = \rho_i/d_i$, where d_i is the density $d_i = N_i/V = x_i d$, V denotes the 2D volume and x_i is the fraction of the i particles (the composition). Now the normalization condition follows

$$\int_0^{\pi} f_i(\phi) d\phi = 1\,. \tag{5}$$

For hard core interactions, the potential U_{ij} is zero if the particles are apart and infinite if the particles overlap. Using this property, we can perform one of the spatial integrations in the formula (3) and obtain the excluded area V_{excl}^{ij}

$$\int \left[e^{-\beta U_{ij}} - 1\right] d\boldsymbol{r}_1 \, d\boldsymbol{r}_2 = -V \, V_{\text{excl}}^{ij}(\phi_1, \phi_2) \, . \tag{6}$$

Using the function f_i and the expression (6), the free energy per particle can be expressed as

$$\begin{aligned} \frac{\beta F}{N} \; = \; & \frac{\beta F_0}{N} \\ & + x_A \int f_A(\phi_1) \left[\log f_A(\phi_1) - 1 + \log \; d_A\right] \; d\phi_1 \\ & + x_B \int f_B(\phi_1) \left[\log f_B(\phi_1) - 1 + \log \; d_B\right] \; d\phi_1 \\ & + \sum_{i,j=A,B} \tfrac{1}{2} x_i x_j d \int V_{\text{excl}}^{ij}(\phi_1, \phi_2) f_i(\phi_1) f_j(\phi_2) d\phi_1 d\phi_2 \, . \end{aligned} \tag{7}$$

2.3. Self-consistency equations and pressure

The minimum condition of the Helmholtz free energy requires that

$$\frac{\delta \left(\beta F/N - \lambda_A \left[\int f_A d\phi - 1\right] - \lambda_B \left[\int f_B d\phi - 1\right]\right)}{\delta f_A} = 0 \, , \tag{8}$$

and

$$\frac{\delta \left(\beta F/N - \lambda_A \left[\int f_A d\phi - 1\right] - \lambda_B \left[\int f_B d\phi - 1\right]\right)}{\delta f_B} = 0 \, , \tag{9}$$

where $\lambda_i, i = A, B$ are the Lagrange multipliers needed here for the normalization conditions to be fulfilled.

For 2D, needles Eq. (8) and Eq. (9) give the following equations

$$\begin{aligned} & \log f_A(\phi_1) = -\log d_A + \lambda_A \\ & - x_A d \int V_{\text{excl}}^{AA}(\phi_1, \phi_2) f_A(\phi_2) d\phi_2 - x_B d \int V_{\text{excl}}^{AB}(\phi_1, \phi_2) f_B(\phi_2) d\phi_2 \, , \end{aligned} \tag{10}$$

$$\begin{aligned} & \log f_B(\phi_1) = -\log d_B + \lambda_B \\ & - x_B d \int V_{\text{excl}}^{BB}(\phi_1, \phi_2) f_B(\phi_2) d\phi_2 - x_A d \int V_{\text{excl}}^{BB}(\phi_1, \phi_2) f_A(\phi_2) d\phi_2 \, , \end{aligned} \tag{11}$$

where

$$V_{\text{excl}}^{ij} = L_i L_j |\sin(\phi_1 - \phi_2)| \,, \tag{12}$$

and where the Lagrange multipliers λ_i can be treated as the chemical potentials μ_i/x_i.

Due to the definition of the pressure P,

$$\beta P = -\frac{\partial \beta F}{\partial V} \,, \tag{13}$$

one can give also an explicit formula for P

$$\beta P = d + \tfrac{1}{2} \sum_{i,j=A,B} d^2 \int V_{\text{excl}}^{ij} f_i(\phi_1) f_j(\phi_2) d\phi_1 d\phi_2 \,. \tag{14}$$

3. Bifurcation analysis

Bifurcation analysis is the simplest and the best tool by the use of which one can gain insight into the possibilities of the structural changes and the symmetries of the new phases. Because of the second order of the transition in the 2D hard needles system, it can directly give the transition points. In the case of liquid crystals, the recommended literature that provides the principles how to perform the bifurcation analysis is given in many papers [31–35].

Following the line of notation from [31], let us rewrite the free energy as

$$\beta F = x_A \langle f_A, \ln f_A \rangle + x_B \langle f_B, \ln f_B \rangle + \tfrac{1}{2} \lambda x_i x_j \sum_{i,j=A,B} \left\langle f_i, K^{ij}[f_j] \right\rangle - \beta\mu_A - \beta\mu_B \,, \tag{15}$$

where $\langle \ldots \rangle = \int \ldots d\phi$, and $K[f] = \int K(\phi_1, \phi_2) f(\phi_2) d\phi_2$. In this notation, λ has the same meaning as the density d.

The minimization condition together with the appropriate normalization leads to the equations

$$f_A = \frac{\exp\left(-\lambda x_A K^{AA}[f_A] - \lambda x_B K^{AB}[f_B]\right)}{\langle 1, \exp\left(-\lambda x_A K^{AA}[f_A] - \lambda x_B K^{AB}[f_B]\right)\rangle} \,, \tag{16}$$

$$f_B = \frac{\exp\left(-\lambda x_B K^{BB}[f_B] - \lambda x_A K^{AB}[f_A]\right)}{\langle 1, \exp\left(-\lambda x_B K^{BB}[f_B] - \lambda x_A K^{AB}[f_A]\right)\rangle} \,, \tag{17}$$

where the terms $K[f]$ play the role of the self consistent "mean field".

To proceed now with the bifurcation analysis, one needs explicit forms of the symmetry adapted functions. As given in [16] for 2D nematic, they take simply the form of $\Delta^n = \cos n\phi$, where $n = 0, 2, 4 \ldots$.

Δ^n's obey the normalization condition

$$\int \Delta^n \Delta^{n'} d\phi = \tfrac{1}{2}\pi\delta_{nn'} \,. \tag{18}$$

The interaction kernels can be cast as a series

$$K^i\left(\widetilde{\phi}\right) = \sum_n \frac{2}{\pi} k_n^i \Delta^n\left(\widetilde{\phi}\right) \,. \tag{19}$$

The symmetry adapted functions fulfill the following mathematical formulas:

$$\int \Delta^n(\phi_1)\Delta^{n'}(\phi_2-\phi_1)d\phi_1 = \tfrac{1}{2}\pi\Delta^n(\phi_2)\delta_{nn'} \,, \tag{20}$$

$$\int K^i(\phi_2-\phi_1)\Delta^n(\phi_1) = \sum_{n'}\int \frac{2}{\pi}k_{n'}^i\Delta^{n'}(\phi_2-\phi_1)\Delta^n(\phi_1)d\phi_1 = \sum_n k_n^i\Delta^n(\phi_2) \,. \tag{21}$$

The main task of the bifurcation analysis is to find the solutions that branch off from the isotropic solution $f_0 = 1/\pi$. In the vicinity of the bifurcation point, the elements of Eq. (16) and Eq. (17) can be expressed in a perturbative manner as expansions in the arbitrary small parameter ε:

$$\begin{aligned} f &= f_0 + \varepsilon f_1 + \varepsilon^2 f_2 \ldots \,, \\ \lambda &= \lambda_0 + \varepsilon\lambda_1 + \varepsilon^2\lambda_2 \ldots \,, \end{aligned} \tag{22}$$

where due to the normalization $< 1, f_k >= 0$ for $k \geq 1$.

Applying formulas of the form like in (22) to Eq. (16) and Eq. (17) and equating terms of the equal order in ε, it is obtained

$$\begin{aligned} &\left(f_0^A + \varepsilon f_1^A\right)\left\langle 1, e^{(-\lambda_0-\varepsilon\lambda_1)\left(x_A K^{AA}\left[f_0^A+\varepsilon f_1^A\right]+x_B K^{AB}\left[f_0^B-\varepsilon f_1^B\right]\right)}\right\rangle \\ &= e^{(-\lambda_0-\varepsilon\lambda_1)\left(x_A K^{AA}\left[f_0^A+\varepsilon f_1^A\right]+x_B K^{AB}\left[f_0^B+\varepsilon f_1^B\right]\right)} \,, \end{aligned} \tag{23}$$

and further

$$\begin{aligned} &f_0^A\left\langle 1, e^{\left(-\lambda_0\left(x_A K^{AA}\left[f_0^A\right]+x_B K^{AB}\left[f_0^B\right]\right)\right)}\right. \\ &\left. e^{\left(-\varepsilon\lambda_1\left(x_A K^{AA}\left[f_0^A\right]+x_B K^{AB}\left[f_0^B\right]\right)-\varepsilon\lambda_0\left(x_A K^{AA}\left[f_1^A\right]+x_B K^{AB}\left[f_1^B\right]\right)\right)}\right\rangle \\ &+ \varepsilon f_1^A\left\langle 1, e^{\left(-\lambda_0\left(x_A K^{AA}\left[f_0^A\right]+x_B K^{AB}\left[f_0^B\right]\right)\right)}\right\rangle \\ &= e^{(-\lambda_0-\varepsilon\lambda_1)\left(x_A K^{AA}\left[f_0^A+\varepsilon f_1^A\right]+x_B K^{AB}\left[f_0^B+\varepsilon f_1^B\right]\right)} \,. \end{aligned} \tag{24}$$

Applying next the expansion $e^x = 1 + x + x^2 + \ldots$ one obtains

$$
\begin{aligned}
&f_0^A \Big\langle 1, e^{\left(-\lambda_0\left(x_A K^{AA}\left[f_0^A\right]+x_B K^{AB}\left[f_0^B\right]\right)\right)} \\
&\left(1-\varepsilon\lambda_1\left(x_A K^{AA}\left[f_0^A\right]+x_B K^{AB}\left[f_0^B\right]\right)-\varepsilon\lambda_0\left(x_A K^{AA}\left[f_1^A\right]+x_B K^{AB}\left[f_1^B\right]\right)\right)\Big\rangle \\
&+\varepsilon f_1^A \left\langle 1, e^{\left(-\lambda_0\left(x_A K^{AA}\left[f_0^A\right]+x_B K^{AB}\left[f_0^B\right]\right)\right)}\right\rangle \\
&= e^{\left(-\lambda_0\left(x_A K^{AA}\left[f_0^A\right]+x_B K^{AB}\left[f_0^B\right]\right)\right)} \\
&\left(1-\varepsilon\lambda_1\left(x_A K^{AA}\left[f_0^A\right]+x_B K^{AB}\left[f_0^B\right]\right)-\varepsilon\lambda_0\left(x_A K^{AA}\left[f_1^A\right]+x_B K^{AB}\left[f_1^B\right]\right)\right) .
\end{aligned}
\tag{25}
$$

The zero order term follows

$$
f_0^A = \frac{e^{\left(-\lambda_0\left(x_A K^{AA}\left[f_0^A\right]+x_B K^{AB}\left[f_0^B\right]\right)\right)}}{\left\langle 1, e^{\left(-\lambda_0\left(x_A K^{AA}\left[f_0^A\right]+x_B K^{AB}\left[f_0^B\right]\right)\right)}\right\rangle}
\tag{26}
$$

and must be equal to $1/\pi$. The first order term, which is of our interest, is

$$
\begin{aligned}
&f_0^A \Big\langle 1, e^{\left(-\lambda_0\left(x_A K^{AA}\left[f_0^A\right]+x_B K^{AB}\left[f_0^B\right]\right)\right)} \\
&\left(-\varepsilon\lambda_1\left(x_A K^{AA}\left[f_0^A\right]+x_B K^{AB}\left[f_0^B\right]\right)-\varepsilon\lambda_0\left(x_A K^{AA}\left[f_1^A\right]+x_B K^{AB}\left[f_1^B\right]\right)\right)\Big\rangle \\
&+\varepsilon f_1^A \left\langle 1, e^{\left(-\lambda_0\left(x_A K^{AA}\left[f_0^A\right]+x_B K^{AB}\left[f_0^B\right]\right)\right)}\right\rangle \\
&= e^{\left(-\lambda_0\left(x_A K^{AA}\left[f_0^A\right]+x_B K^{AB}\left[f_0^B\right]\right)\right)} \\
&\left(-\varepsilon\lambda_1\left(x_A K^{AA}\left[f_0^A\right]+x_B K^{AB}\left[f_0^B\right]\right)-\varepsilon\lambda_0\left(x_A K^{AA}\left[f_1^A\right]+x_B K^{AB}\left[f_1^B\right]\right)\right) .
\end{aligned}
\tag{27}
$$

First term on the left-hand side and first term on the right-hand side of Eq. (27), taking into account Eq. (26), are equal to each other. Also averages (like $\langle 1, f_1\rangle = 0$) from the perturbation terms must vanish, so finally one obtains

$$
\begin{aligned}
&\varepsilon f_1^A \left\langle 1, e^{\left(-\lambda_0\left(x_A K^{AA}\left[f_0^A\right]+x_B K^{AB}\left[f_0^B\right]\right)\right)}\right\rangle \\
&= e^{\left(-\lambda_0\left(x_A K^{AA}\left[f_0^A\right]+x_B K^{AB}\left[f_0^B\right]\right)\right)} \\
&\left(-\varepsilon\lambda_0\left(x_A K^{AA}\left[f_1^A\right]+x_B K^{AB}\left[f_1^B\right]\right)\right) .
\end{aligned}
\tag{28}
$$

Rewriting this formula as

$$
f_1^A = \left(-\lambda_0\left(x_A K^{AA}\left[f_1^A\right]+x_B K^{AB}\left[f_1^B\right]\right)\right) \frac{e^{\left(-\lambda_0\left(x_A K^{AA}\left[f_0^A\right]+x_B K^{AB}\left[f_0^B\right]\right)\right)}}{\left\langle 1, e^{\left(-\lambda_0\left(x_A K^{AA}\left[f_0^A\right]+x_B K^{AB}\left[f_0^B\right]\right)\right)}\right\rangle}
\tag{29}
$$

and taking into account that uniform isotropic distributions like Eq. (26) are equal to $1/\pi$ the bifurcation formulas are finally obtained as

$$\begin{aligned} f_1^A &= \left(-\lambda_0 \left(x_A K^{AA}\left[f_1^A\right] + x_B K^{AB}\left[f_1^B\right]\right)\right)\frac{1}{\pi}\,, \\ f_1^B &= \left(-\lambda_0 \left(x_B K^{BB}\left[f_1^B\right] + x_A K^{AB}\left[f_1^A\right]\right)\right)\frac{1}{\pi}\,. \end{aligned} \tag{30}$$

The first two terms of the ODF functions are

$$\begin{aligned} f^A &= a_0 + a_2 \Delta_2\,, \\ f^B &= b_0 + b_2 \Delta_2\,, \end{aligned} \tag{31}$$

so $f_1^A = a_2\Delta_2$ and $f_1^B = b_2\Delta_2$, and

$$\begin{aligned} K^{AA}\left[f_1^A\right] &= a_2 \int K^{AA}\left(\phi_2 - \phi_1\right)\Delta_2\left(\phi_1\right) d\phi_1 = a_2 \sum_n k_n^{AA} \Delta_2(\phi_2)\,, \\ K^{BB}\left[f_1^B\right] &= b_2 \int K^{BB}\left(\phi_2 - \phi_1\right)\Delta_2(\phi_1) d\phi_1 = b_2 \sum_n k_n^{BB} \Delta_2(\phi_2)\,. \end{aligned} \tag{32}$$

The set of the bifurcation equation emerges from Eq. (30) as

$$\begin{aligned} a_2\Delta_2 &= -\frac{\lambda_0}{\pi}\left(a_2 x_A k_2^{AA}\Delta_2 + b_2 x_B k_2^{AB}\Delta_2\right)\,, \\ b_2\Delta_2 &= -\frac{\lambda_0}{\pi}\left(b_2 x_B k_2^{BB}\Delta_2 + a_2 x_A k_2^{AB}\Delta_2\right)\,. \end{aligned} \tag{33}$$

To get rid of the functional form, we can multiply both sides by Δ_2 and integrate over the angle ϕ

$$\begin{aligned} a_2 &= -\frac{\lambda_0}{\pi}\left(a_2 x_A k_2^{AA} + b_2 x_B k_2^{AB}\right)\,, \\ b_2 &= -\frac{\lambda_0}{\pi}\left(b_2 x_B k_2^{BB} + a_2 x_A k_2^{AB}\right)\,. \end{aligned} \tag{34}$$

From this set of equations, one obtains the relation

$$\frac{x_B k_2^{AB}}{-\pi/\lambda_0 - x_B k_2^{BB}} = \frac{-\pi/\lambda_0 - x_A k_2^{AA}}{x_A k_2^{AB}} \tag{35}$$

which is a square equation for the unknown λ_0

$$x_A x_B \left(k_2^{AB}\right)^2 = \left(\frac{\pi}{\lambda_0}\right)^2 + \frac{\pi}{\lambda_0}\left(x_A k_2^{AA} + x_B k_2^{AB}\right) + x_A k_2^{AA} x_B k_2^{BB}\,. \tag{36}$$

From this equation, one obtains finally the expression for the bifurcation point density

$$\frac{2\pi}{\lambda_{\rm bif}^{1,2}} = -\left(x_A k_2^{AA} + x_B k_2^{BB}\right) \pm \sqrt{\left(x_A k_2^{AA} + x_B k_2^{BB}\right)^2 - 4x_A x_B \left(k_2^{AA} k_2^{BB} - k_2^{AB} k_2^{AB}\right)} \,. \tag{37}$$

For the Onsager particles interacting accordingly to the formula $K(\widetilde{\phi}) = L_i L_j |\sin(\widetilde{\phi})|$, the needed coefficients are $k_2^{ij} = -L_i L_j \frac{2}{3}, k_4^{ij} = -L_i L_j \frac{2}{15}, k_6^{ij} = -L_i L_j \frac{2}{35}$.

If we put that the particles are of the same kind then from the formula Eq. (37), one obtains the known expression for the monodispersed system

$$\frac{\pi}{\lambda_{\rm bif}} = -k_2 \,. \tag{38}$$

4. Results, applications and perspectives

The formalism presented in the previous section has been used to obtain the phase diagram for a binary mixture of two-dimensional system, which because of the only one anisotropic phase — nematic phase, is simplified. In Fig. 2, the transition line is given that separates the isotropic from the

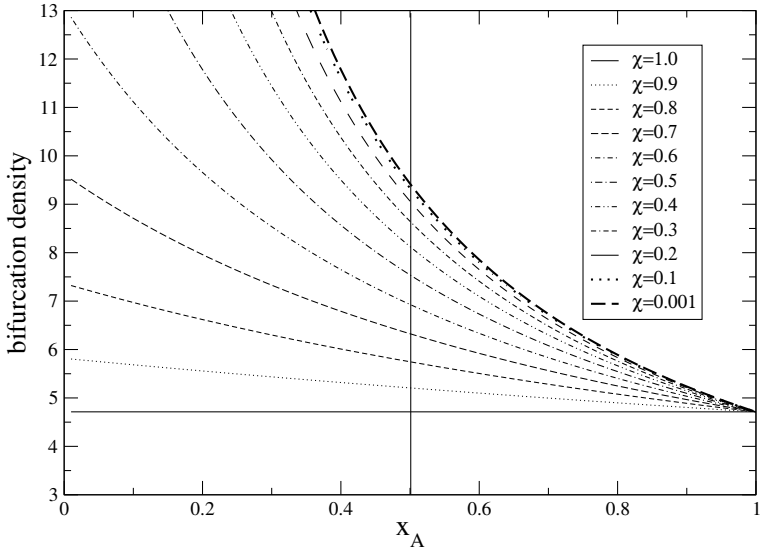

Fig. 2. Density of the bifurcation, $\rho^* = \rho L_A^2$, *versus* composition x_A obtained for different values of χ.

nematic phase *versus* composition x_A. The monodispersed system is represented here by the straight bottom line at $\rho^* = 4.71$. The length difference between the needle A and B describes the coefficient $\chi = L_A/L_B$. At the left side of the diagram, the bifurcation lines reach the values of the density bifurcation for a pure B system, and at the right side — the A system. The lines connecting these points are, however, far from linear. It is noticeable that its character is dominated by the longer needles — the curves are bent downwards with the curvature apparently depending on $\chi = L_A/L_B$.

If the particles B are as short, that they can be regarded as dots one still observes the transition line (thick dashed lines in Fig. 2 and Fig. 3), which escapes to infinity if the composition $x_A - > 0$. Yet at the composition $x_A = 0.5$, which corresponds to the mixture composed of 50 percent of the needles and 50 percent of the dot-like objects, the bifurcation density is not very much increased — it is $\rho^* = 9.12$, which is about twice the density of the pure needles system. While diminishing the number of the hard lines as compared to the dots, below $x_A = 0.5$, the area of the isotropic phase rapidly increases. Fig. 3 presents a part of the phase diagram at very small numbers of x_A. One sees that for the anisotropy ratio $\chi > 0.5$ all the density lines of the bifurcation are smaller than $\rho^* = 20$, *i.e.* 5 times larger than the transition density of the pure needle system.

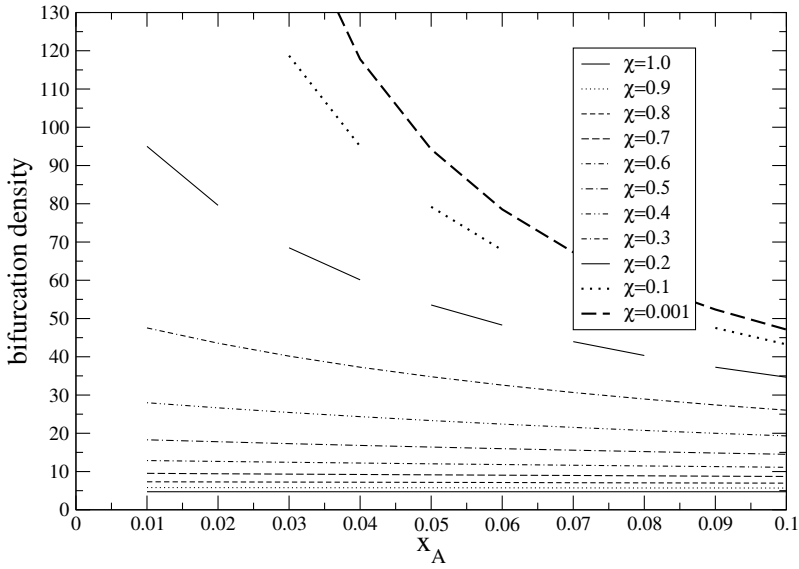

Fig. 3. Density of the bifurcation, $\rho^* = \rho L_A^2$, *versus* composition x_A obtained for different values of χ.

Let us assume now a binary mixture, where the coefficients of the molecules of the type A are $k_2^{AA} = -L_A L_A \frac{2}{3}$ and of the type B $k_2^{BB} = -L_B L_B \frac{2}{3}$, but their mutual preferred orientations are perpendicular according, for instance, to the potential of the form $K^{AB} = L_A L_B |\cos(\varphi)|$ leading to the coefficient $k_2^{AB} = L_A L_B \frac{2}{3}$. This condition may seem a bit unrealistic at first glance, although some suggestions toward obtaining similar situation would be to add the dipol interactions, for the particle A along their orientation and for the particles B — perpendicularly. On the theoretical grounds, however, any strength can be considered just to observe the properties produced by the equations of interest.

First observation, which is a bit surprising, is that due to the structure of the Eq. (37), the bifurcation lines will be exactly the same. The possible differences may occur in the order parameters.

In Fig. 4 and Fig. 5, an influence of the cross term on the phase diagram is presented. Figure 4 shows the situation when the parameter $k_2^{AB}(\text{modified}) = \alpha k_2^{AB}$ is gradually diminished while the particles A and B are kept the same. It causes and increase in the bifurcation density with the maximum at $x_A = 0.5$ and while the term vanishes this maximum takes the form of a cusp at the level twice higher than the original bifurcation density $\rho^* = 4.71$. Figure 5, on the other hand, presents the effect of strengthening of the interaction cross term. It substantially lowers the bifurcation density profiles, dominating the influence of K_{AA} and K_{BB} terms.

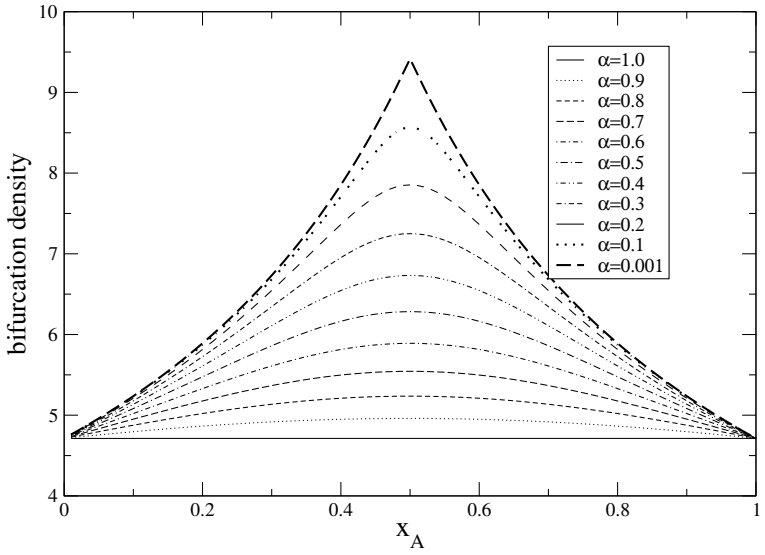

Fig. 4. Density of the bifurcation, $\rho^* = \rho L_A^2$, *versus* composition x_A obtained for different values of α.

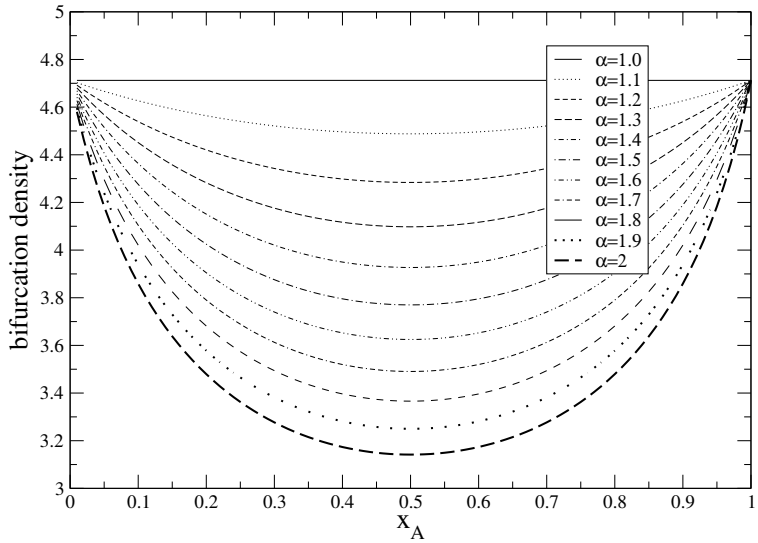

Fig. 5. Density of the bifurcation, $\rho^* = \rho L_A^2$, *versus* composition x_A obtained for different values of α.

All the above profiles can be useful as a guide for studying the problem of adsorption of long rod-like molecules at surfaces. An example of such process is the adsorption of fibrinogen [36, 37], which has been recently intensively studied because of its possible medical applications for the surfaces of the implants. Fibrinogen is a soluble plasma glycoprotein that is converted by thrombin into fibrin during blood coagulation. As far as human body is concerned it is biologically friendly. Other applications of protein coverages, especially structured, indicate their high potential also for pharmaceuticals, cosmetics industries and food sciences [38].

In the studies of adsorption, a crucial subject is then a two-dimensional ordered arrangement. In the experiments with fibrinogen, the molecules are being adsorbed from a liquid solution onto the solid surface. As a result, some molecules are adsorbed as lying flat on the surface, the rest are being attached to it only with one of the ends and protrude from the surfaces. The arrangement of the molecules within the plane can be regarded then as a binary mixture of rod-like molecules and small spheres.

Generally, the process of adsorption concerns a random packing problem which, in principle, despite the fact that it depends on the solution properties like composition, features of the solid surface and the kinetics itself, it produces an isotropic arrangement. Newly adsorbed molecules increase surface density till a saturated value is obtained. To still accept particles the layer of the adsorbed particles must have the possibility to reorient. If the particles can reorient, which process is not obvious from experiment, then one may even talk about thermodynamically stable 2d phases.

The current paper on needles provides the limits for the particles density to obtain an ordered phase. Since there is no much difference between interactions of a long needle with a very short needle and a long needle and an appropriately small sphere, one can even expect that the above given limits can be of help to explain experimental results for fibrinogen adsorption. Besides this example, the model refers also to a number of a many types of 2D binary mixtures.

REFERENCES

[1] J.M. Kosterlitz, D. Thouless, *J. Phys. C* **6**, 1181 (1973).

[2] R.E. Peierls, *Helv. Phys. Acta* **7**, 81 (1934); *Ann. Inst. Henri Poincare* **5**, 177 (1935).

[3] F. Bloch, *Z. Phys.* **61**, 206 (1930).

[4] P.G. de Gennes, J. Prost, *The Physics of Liquid Crystals*, OUP, 1993.

[5] N.D. Mermin, H. Wagner, *Phys. Rev. Lett.* **17**, 1133 (1966); P.C. Hohenberg, *Phys. Rev.* **158**, 383 (1967); N.D. Mermin, *Phys. Rev.* **176**, 250 (1968).

[6] J.P. Straley, *Phys. Rev.* **A4**, 675 (1971); M. Romeiro, *J. Math. Phys.* **19**, 802 (1978); P.A. Vullermot, M. Romeiro, *Commun. Math. Phys.* **41**, 281 (1975).

[7] T.F. Keller *et al.*, *ACS NANO* **5**, 3120 (2011).

[8] J. Zemla, J. Rysz, A. Budkowski, K. Awsiuk, *Soft Matter* **8**, 5550 (2012).

[9] J.M. Deutsch, M. Warkentin, *Phys. Rev. Lett.* **95**, 257802 (2005).

[10] J.D. Parsons, *Phys. Rev.* **A19**, 1225 (1979).

[11] S.-D. Lee, *J. Chem. Phys.* **87**, 4972 (1987); S.-D. Lee, *J. Chem. Phys.* **89**, 7036 (1988).

[12] B. Barboy, W.M. Gelbart, *J. Chem. Phys.* **71**, 3053 (1979).

[13] D. Frenkel, R. Eppenga, *Phys. Rev.* **A31**, 1776 (1985).

[14] A. Chrzanowska, H. Ehrentraut, *Tech. Mechanik* **22**, 56 (2002).

[15] A. Chrzanowska, H. Ehrentraut, *Phys. Rev.* **E66**, 012201 (2002).

[16] A. Chrzanowska, *Acta Phys. Pol. B* **36**, 3163 (2005).

[17] R.F. Kayser, H.J. Raveche, *Phys. Rev.* **A17**, 2067 (1978).

[18] A. Poniewierski, *Phys. Rev.* **E47**, 3396 (1993).

[19] A. Poniewierski, R. Holyst, *Phys. Rev.* **A38**, 3721 (1988).

[20] Y. Mao, P. Bladon, H.N.W. Lekkerkerker, M.E. Cates, *Mol. Phys.* **92**, 151 (1997).

[21] R.L.C. Vink, *Eur. Phys. J.* **B72**, 225 (2009).

[22] D. Frenkel, J.F. Maguire, *Phys. Rev. Lett.* **47**, 1025 (1981).

[23] A. Chrzanowska, *J. Chem. Phys.* **120**, 2857 (2004).

[24] A. Mukoyama, Y. Yoshimura, *J. Phys. A* **30**, 6667 (1997).

[25] A. Chrzanowska, H. Ehrentraut, in: *Dynamic Response of Granular and Porous Materials under Large and Catastrophic Deformations*, Springer, 2003, p. 315.

[26] D. Frenkel, J.F. Maguire, *Mol. Phys.* **49**, 503 (1983).

[27] M.E. Foulaadvand, M. Yarifard, *Eur. Phys. J.* **E34**, 41 (2011).

[28] M.C. Lagomarsino, M. Dogterom, M. Dijkstra, *J. Chem. Phys.* **119**, 3535 (2003).

[29] L. Onsager, *Ann. N.Y. Acad. Sci.* **51**, 627 (1949).

[30] J. Stecki, A. Kloczkowski, *J. Phys.* **40**, 360 (1979).

[31] B. Mulder, *Phys. Rev.* **A39**, 360 (1989).

[32] L. Longa, *J. Chem. Phys.* **85**, 2974 (1986).

[33] A. Chrzanowska, *Phys. Rev.* **E58**, 3229 (1998).

[34] L. Longa, *Z. Phys.* **B85**, 357 (1986).

[35] L. Longa, *Liq. Cryst.* **5**, 443 (1989).

[36] Z. Adamczyk, J. Barbasz, M. Cieśla, *Langmuir* **27**, 6868 (2011).

[37] Z. Adamczyk, J. Barbasz, M. Cieśla, *Langmuir* **26**, 11934 (2010).

[38] P. Kalchevsky, K. Nagayama (Eds.), *Particles at Fluid Interfaces and Membranes, Attachment of Colloid Particles and Proteins to Interfaces and Formation of Two-Dimensional Arrays*, Elsevier Science and Technology, 2001.